Neuron, Volume *97*

Supplemental Information

Drd3 Signaling in the Lateral Septum Mediates Early Life Stress-Induced Social Dysfunction

Sora Shin, Horia Pribiag, Varoth Lilascharoen, Daniel Knowland, Xiao-Yun Wang, and Byung Kook Lim

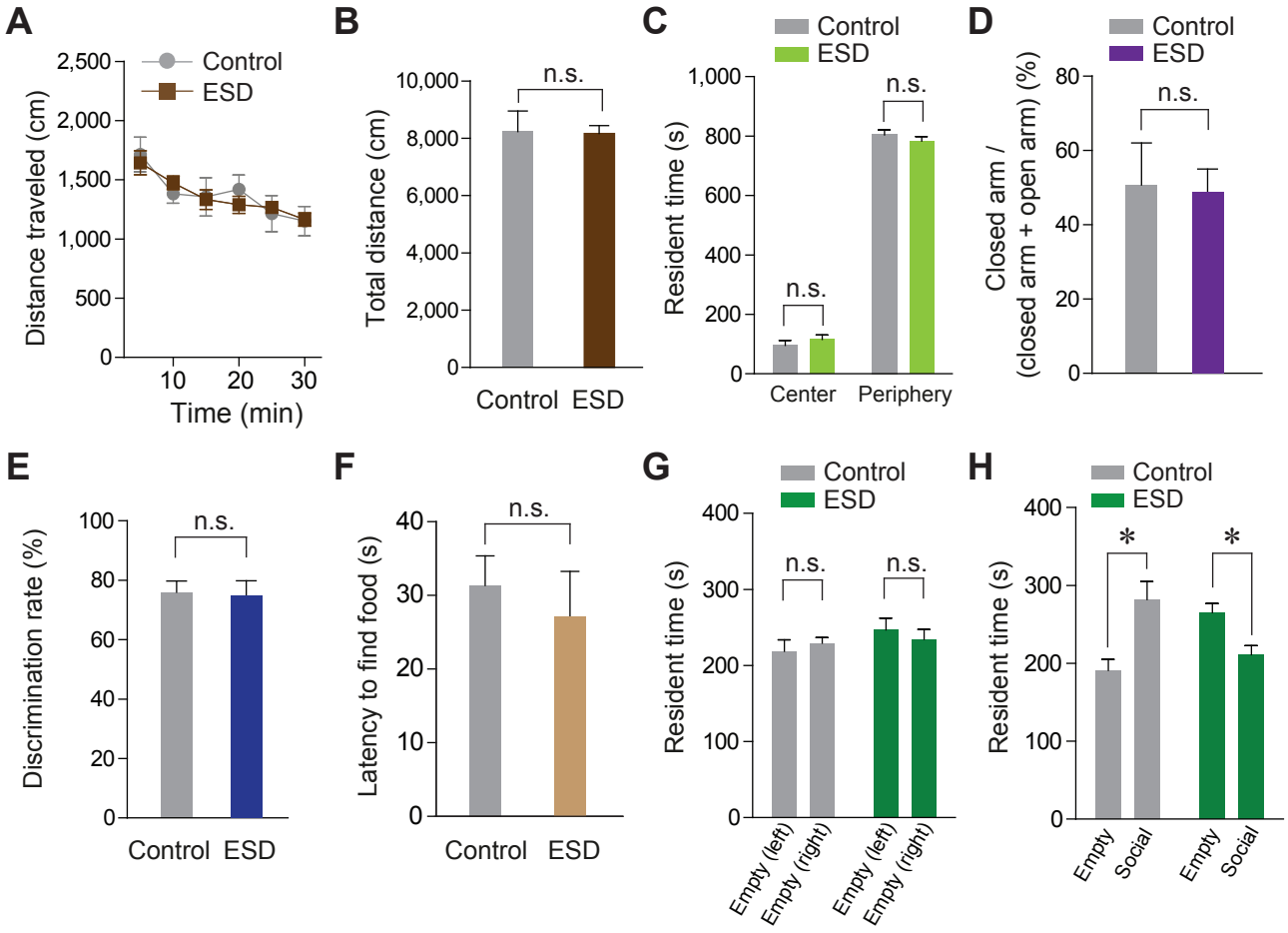
A
Control
ESD
Distance traveled (cm)
2,500
2,000
1,500
1,000
500
0
10
20
30
Time (min)
B
Total distance (cm)
10,000
8,000
6,000
4,000
2,000
0
n.s.
Control
ESD
C
Control
ESD
Resident time (s)
1,000
800
600
400
200
0
n.s.
n.s.
Center
Periphery
D
Control
ESD
Closed arm /
(closed arm + open arm) (%)
80
60
40
20
0
n.s.
E
Discrimination rate (%)
100
80
60
40
20
0
n.s.
Control
ESD
F
Latency to find food (s)
40
30
20
10
0
n.s.
Control
ESD
G
Control
ESD
Resident time (s)
400
300
200
100
0
n.s.
n.s.
Empty (left)
Empty (right)
Empty (left)
Empty (right)
H
Control
ESD
Resident time (s)
400
300
200
100
0
*
*
Empty
Social
Empty
Social

Figure S1

Figure S1. Basic Characteristics of ESD mice, Related to Figure 1

(A and B) Locomotor activity was monitored for 30 min and analyzed in 5 min-bins (A) and total distance traveled was measured during the 30 min test period (B). No significant difference in locomotion was observed between control and ESD mice (n = 5 per group).

(C) The resident time spent in the center or periphery of the open field. ESD mice showed normal levels of anxiety-like behaviors comparable to control mice in the open field test (n = 9, 11 mice per group).

(D) Percentage time spent in the closed arms of elevated plus-maze. ESD mice had no observable anxiety in the elevated plus maze (n = 4, 6 mice per group).

(E) Novel object recognition test. ESD mice showed the regular ability to recognize a novel object (n = 9 per group).

(F) Buried food olfactory test. No significant difference in latency to find buried food was observed between control and ESD mice (n = 9, 8 mice per group).

(G) The habituation session of three-chamber test. No side preference was apparent during the habitation for control and ESD mice (n = 7, 11 mice per group).

(H) The test session of three-chamber test. Control mice spent more time in the side designated as the ‘social’ than the ‘empty’ compartment, whereas ESD mice did not show preferences for social compartment (n = 7, 11 mice per group).

Significance for multiple comparisons: Paired *t*-test [(H)], $*P < 0.05$. n.s., not significant. Data are presented as mean ± s.e.m.

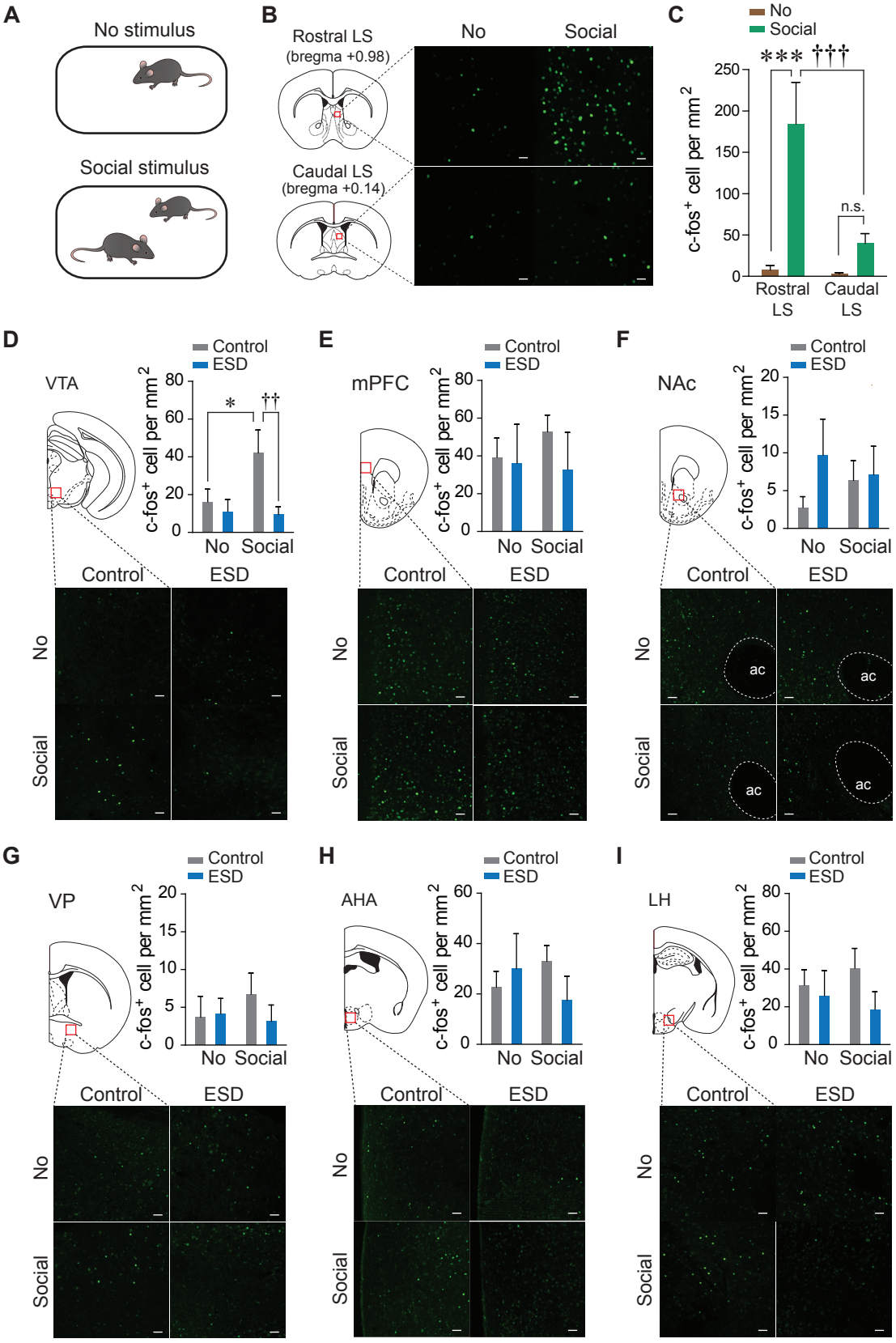
A
No stimulus
Social stimulus
B
Rostral LS
(bregma +0.98)
Caudal LS
(bregma +0.14)
No
Social
C
No
Social
***
†††
n.s.
c-fos+ cell per mm2
Rostral LS
Caudal LS
D
VTA
Control
ESD
*
††
No
Social
E
mPFC
F
NAc
ac
G
VP
H
AHA
I
LH

Figure S2

Figure S2. Quantification of c-fos-positive Cells in the Several Brain Areas Following Exposure to Social Stimulus, Related to Figure 1

(A) Schematics illustrating the experimental design for examining c-fos induction by social stimulus.

(B) Representative images of the rostral and caudal LS of control mice showing c-fos expression following exposure to a social stimulus. Scale bars, 20 μm.

(C) Quantifications of c-fos-positive cells in the rostral and caudal LS. Social stimulus elicited a robust increase of c-fos expression in the rostral LS compared to the caudal LS (n = 6 mice for each no stimulus group and n = 5 mice for each social stimulus group).

(D to I) Quantifications (top) and representative images (bottom) of c-fos-positive cells in the VTA (D), mPFC (E), NAc (F), VP (G), AHA (H) and LH (I) between control and ESD mice after exposure to a social stimulus. Social stimulus induces a robust c-fos expression in the VTA (D) of control, but not of ESD mice (n = 6 mice for each no stimulus group and n = 7 mice for each social stimulus group). No changes in c-fos-positive cells within the mPFC, NAc, VP, AHA and LH. Scale bars, 50 μm. ac, anterior commissure.

Significance for multiple comparisons: Two-way RM ANOVA; post-hoc, Fisher LSD [(C)], and Two-way ANOVA; post-hoc, Bonferroni [(D)], $^{*}P < 0.05$; $^{***}P < 0.001$; $^{\dagger\dagger}P < 0.01$; $^{\dagger\dagger\dagger}P < 0.001$; n.s., not significant. Data are presented as mean ± s.e.m.

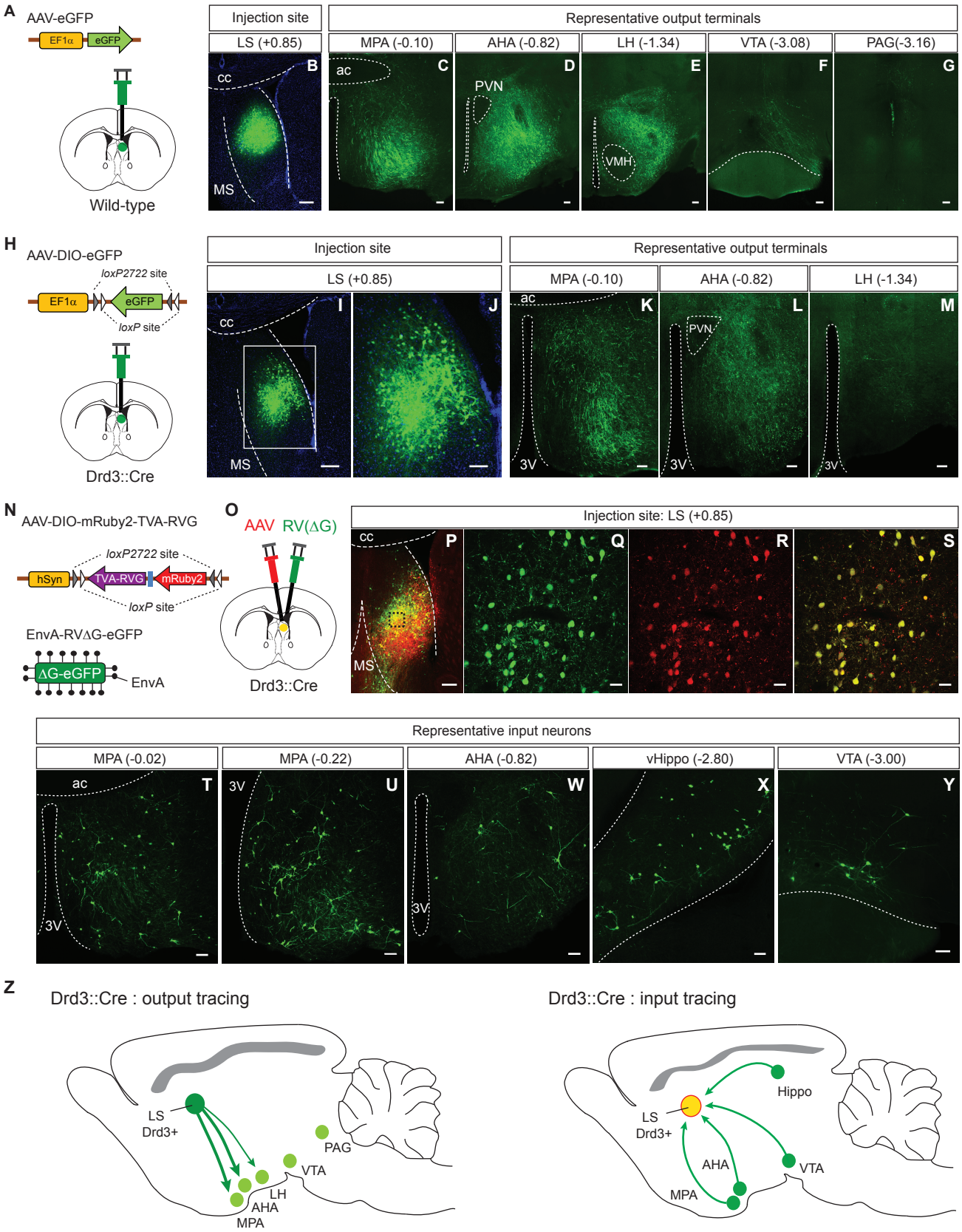
A
AAV-eGFP
EF1α
eGFP
Wild-type
Injection site
Representative output terminals
LS (+0.85)
MPA (-0.10)
AHA (-0.82)
LH (-1.34)
VTA (-3.08)
PAG(-3.16)
B
C
D
E
F
G
cc
ac
PVN
VMH
MS
H
AAV-DIO-eGFP
loxP2722 site
loxP site
Drd3::Cre
I
J
K
L
M
3V
N
AAV-DIO-mRuby2-TVA-RVG
hSyn
TVA-RVG
mRuby2
EnvA-RVΔG-eGFP
ΔG-eGFP
EnvA
O
AAV
RV(ΔG)
Injection site: LS (+0.85)
P
Q
R
S
Representative input neurons
MPA (-0.02)
MPA (-0.22)
AHA (-0.82)
vHippo (-2.80)
VTA (-3.00)
T
U
W
X
Y
Z
Drd3::Cre : output tracing
Drd3::Cre : input tracing
LS
Drd3+
PAG
VTA
LH
AHA
MPA
Hippo

Figure S3

Figure S3. The Afferent and Efferent Connections of Drd3^{LS} neurons, Related to Figure 2

(A) Schematic illustrating the injection of AAV expressing eGFP into the LS of wild-type mice.

(B) The image shows a robust eGFP expression in the LS cell bodies without cell-type specificity. Scale bar, 200 μm. cc, corpus callosum; MS, medial septum.

(C to G) eGFP-positive axons from LS cell bodies were found in the MPA (C), AHA (D), LH (E), VTA (F), and PAG (G). Scale bars, 100 μm. ac, anterior commissure; PVN, paraventricular nucleus; VMH, ventromedial hypothalamus.

(H) Schematic illustrating the injection of AAV expressing eGFP in a Cre-dependent manner into the LS of Drd3::Cre mice.

(I and J) The image showing robust eGFP expression in the Drd3^{LS} neuronal cell bodies (I), and its high magnification image (J). Scale bars, 200 μm, 100 μm, respectively.

(K to M) eGFP-positive axons from Drd3^{LS} cell bodies were found in the MPA (K), AHA (L), and LH (M). Scale bars, 100 μm. PVN, paraventricular nucleus; 3V, third ventricle.

(N and O) Schematic showing the strategy for rabies-mediated retrograde tracing of monosynaptic inputs to Drd3^{LS} neurons. Two different viruses were used. AAV expressing both EnvA receptor (TVA) and rabies virus glycoprotein (RVG) in a Cre-dependent manner (AAV-DIO-mRuby2-TVA-RVG); EnvA-pseudotyped glycoprotein (G)-deleted rabies virus expressing eGFP (EnvA-RVΔG-eGFP) (N). AAV-DIO-mRuby2-TVA-RVG was firstly injected into the LS of Drd3::Cre mice. Two weeks later, EnvA-RVΔG-eGFP was injected again into the same site (O).

(P) The confocal image showing starter cells (yellow, expressing both eGFP and mRuby2) in the LS of Drd3::Cre mice. Scale bar, 200 μm.

(Q to S) Enlarged views of a region in the black dotted box showing in (P). Green, expressing eGFP (Q); Red, expressing mRuby2 (R); Yellow, expressing both eGFP and mRuby2 (S). Scale bars, 30 μm.

(T to Y) Images showing rabies-labelled presynaptic neurons in the rostral and caudal part of MPA (T and U, respectively), AHA (W), vHippo (X), and VTA (Y). Scale bars, 100 μm.

(Z) Schematic summary of the brain regions that receive $Drd3^{LS}$ neuronal projections (left) and that provide inputs to $Drd3^{LS}$ neurons (right).

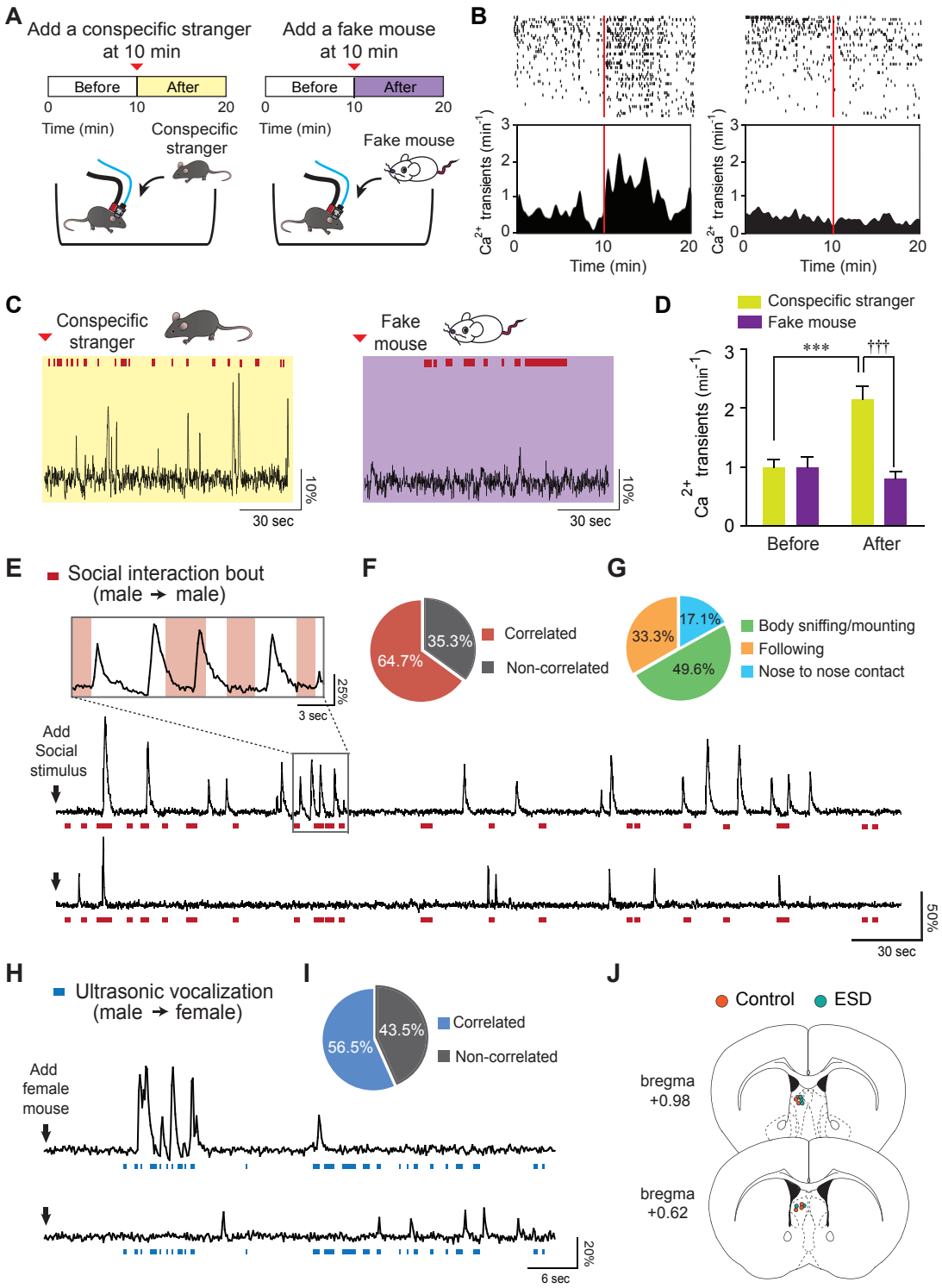
A
Add a conspecific stranger at 10 min
Before
After
0
10
20
Time (min)
Conspecific stranger
Add a fake mouse at 10 min
Before
After
0
10
20
Time (min)
Fake mouse
B
Ca2+ transients (min-1)
Time (min)
C
Conspecific stranger
Fake mouse
10%
30 sec
D
Conspecific stranger
Fake mouse
***
†††
Ca2+ transients (min-1)
Before
After
E
Social interaction bout (male → male)
25%
3 sec
Add Social stimulus
50%
30 sec
F
35.3%
64.7%
Correlated
Non-correlated
G
17.1%
33.3%
49.6%
Body sniffing/mounting
Following
Nose to nose contact
H
Ultrasonic vocalization (male → female)
Add female mouse
20%
6 sec
I
43.5%
56.5%
Correlated
Non-correlated
J
Control
ESD
bregma +0.98
bregma +0.62

Figure S4

Figure S4. *In vivo* Imaging of Ca^{2+} Dynamics from $Drd3^{LS}$ Neurons of Control Drd3::Cre Mice during Social Interaction, Related to Figure 3

(A) Schematic for *in vivo* imaging of Ca^{2+} dynamics in $Drd3^{LS}$ neurons of control Drd3::Cre mice. Images for fluorescently encoded Ca^{2+} transients were acquired before and after the presentation of either a conspecific stranger (left) or a fake mouse (right).

(B) Raster plots (top) and peristimulus time histograms (bottom) showing $Drd3^{LS}$ neuronal activity of control Drd3::Cre mice in response to either a conspecific stranger (left, n = 44 cells from 3 mice) or a fake mouse (right, n = 48 cells from 4 mice). The rows and ticks in the raster plots represent individual cells and single Ca^{2+} transient events, respectively. Vertical red bars mark the time the conspecific stranger or fake mouse was introduced.

(C) Representative Ca^{2+} activity traces from $Drd3^{LS}$ neurons of control Drd3::Cre mice after presenting of a conspecific stranger (left) or a fake mouse (right), respectively. Red dashed areas indicate physical interaction bouts with a conspecific stranger or a fake mouse.

(D) Normalized average Ca^{2+} transients per min in $Drd3^{LS}$ neurons of control Drd3::Cre mice before and after the presentation of a conspecific stranger or a fake mouse (n = 44 cells from 3 mice for conspecific strangers, n = 48 cells from 4 mice for fake mice).

(E) Example traces of $Drd3^{LS}$ neuronal activity from two representative cells during male to male social interaction. Red dashed areas indicate social interaction bouts. Zoom-in of gray box (top) showed relating GCaMP6f signal of a $Drd3^{LS}$ neuron below with light red shaded areas indicating social interaction.

(F and G) Pie charts indicate percentage of Ca^{2+} transient events from $Drd3^{LS}$ neurons of control Drd3::Cre mice correlating with social interaction bouts (F) and with different subtypes of social interaction behaviors (G) during the first 2 min-recording after introducing a male intruder (n = 33 cells from 3 mice).

(H) Example traces of $Drd3^{LS}$ neuronal activity from two representative cells during USV tests. A female mouse was added for recording USVs produced by male experimental mice. Blue dashed areas indicate the generation of USVs.

(I) Pie charts indicate percentage of Ca^{2+} transient events from $Drd3^{LS}$ neurons of control Drd3::Cre mice correlating with USVs during the first 1-min recording after introducing a female intruder (n = 26 cells from 3 mice).

(J) Locations of the GRIN lens in the Drd3::Cre mice included in Figures 3G to 3J. Symbols represent the different groups: orange circle, control Drd3::Cre mice; blue circle, ESD Drd3::Cre mice.

Significance for multiple comparisons: Two-way RM ANOVA; post-hoc, Fisher LSD [(D)], $^{***}P < 0.001$; $^{\dagger\dagger\dagger}P < 0.001$. Data are presented as mean ± s.e.m.

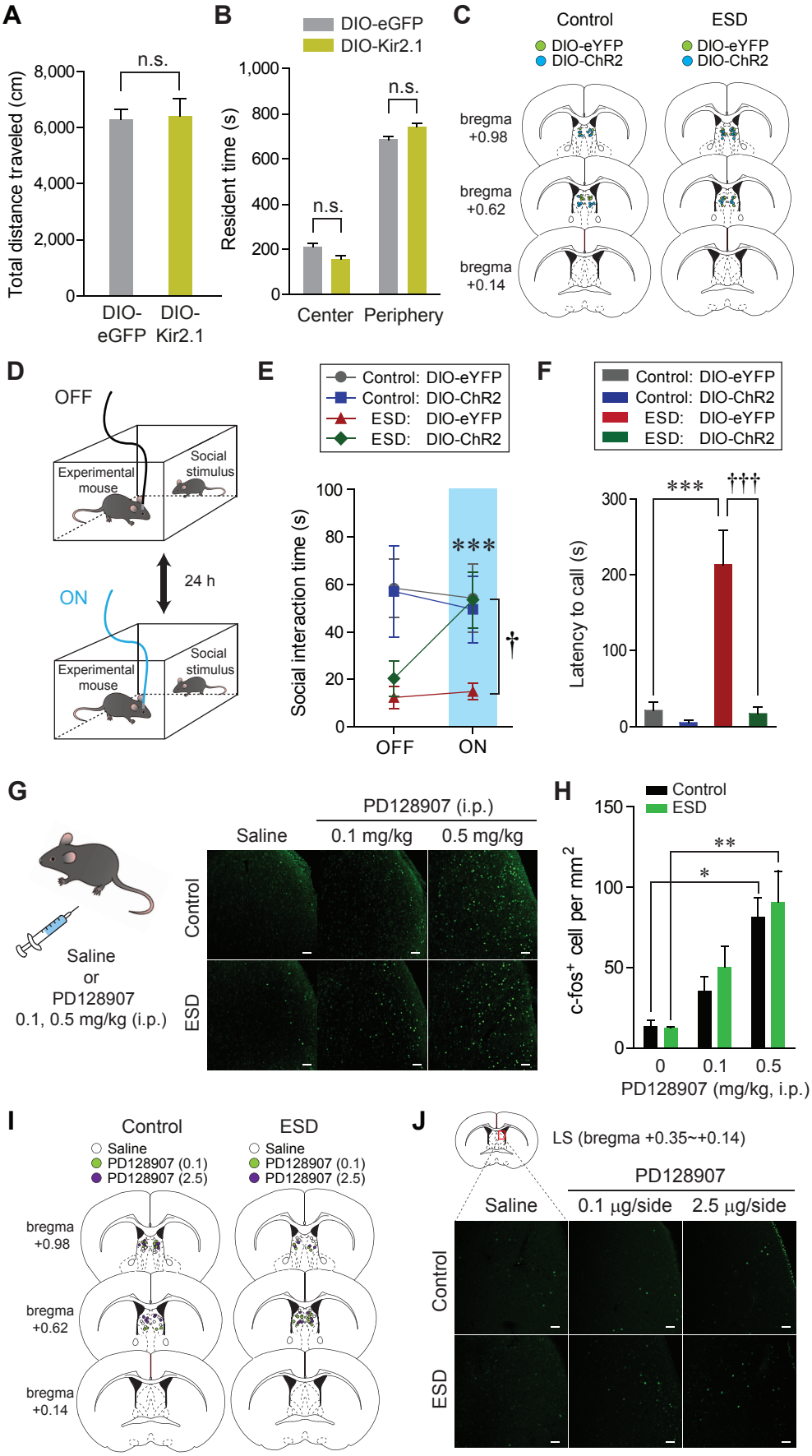
A
Total distance traveled (cm)
8,000
6,000
4,000
2,000
0
n.s.
DIO-eGFP
DIO-Kir2.1
B
DIO-eGFP
DIO-Kir2.1
Resident time (s)
1,000
800
600
400
200
0
n.s.
n.s.
Center
Periphery
C
Control
ESD
DIO-eYFP
DIO-ChR2
DIO-eYFP
DIO-ChR2
bregma +0.98
bregma +0.62
bregma +0.14
D
OFF
Experimental mouse
Social stimulus
24 h
ON
Experimental mouse
Social stimulus
E
Control: DIO-eYFP
Control: DIO-ChR2
ESD: DIO-eYFP
ESD: DIO-ChR2
Social interaction time (s)
100
80
60
40
20
0
***
†
OFF
ON
F
Control: DIO-eYFP
Control: DIO-ChR2
ESD: DIO-eYFP
ESD: DIO-ChR2
Latency to call (s)
300
200
100
0
***
†††
G
Saline
or
PD128907
0.1, 0.5 mg/kg (i.p.)
PD128907 (i.p.)
Saline
0.1 mg/kg
0.5 mg/kg
Control
ESD
H
Control
ESD
c-fos+ cell per mm2
150
100
50
0
**
*
0
0.1
0.5
PD128907 (mg/kg, i.p.)
I
Control
ESD
Saline
PD128907 (0.1)
PD128907 (2.5)
Saline
PD128907 (0.1)
PD128907 (2.5)
bregma +0.98
bregma +0.62
bregma +0.14
J
LS (bregma +0.35~+0.14)
PD128907
Saline
0.1 μg/side
2.5 μg/side
Control
ESD

Figure S5

Figure S5. Modulation of Drd3^{LS} Neuronal Activity affects ESD-induced Abnormal Social Behaviors and Pharmacological Activation of Drd3 signaling Increases LS Neuronal Activity, Related to Figures 4 and 5

(A) Total distance traveled during the 15-min locomotion test. Viral-mediated Kir2.1 expression in the Drd3^{LS} neurons of control Drd3::Cre mice did not alter the locomotion (n = 3, 4 mice per group).

(B) Injection of the AAV-DIO-Kir2.1 into the LS of control Drd3::Cre mice had no effects on anxiety-like behaviors in open field tests (n = 3, 4 mice per group).

(C) Locations of the optic fibers in Drd3::Cre mice included in Figures 4I, 4K. Symbols represent the different groups: light green circle, AAV-DIO-eYFP; blue circle, AAV-DIO-ChR2.

(D) The experimental design of reciprocal social interaction tests with optical stimulations. Five-minutes testing sessions were conducted twice and counterbalanced for order with a 24 h interval between laser ON and laser OFF conditions.

(E) Photoactivation of Drd3^{LS} neurons rescued the amount of time ESD Drd3::Cre mice spent in direct social interaction (sniffing, following, mounting and nose to nose contacts) to the levels of control Drd3::Cre mice (n = 5, 6 mice for each control group and n = 6, 6 mice for each ESD group; ***$P < 0.001$ compared with ESD mice expressing DIO-ChR2 at OFF state; $^{\dagger}P < 0.05$ compared with ESD mice expressing DIO-eYFP at ON state).

(F) Photoactivation of Drd3^{LS} neurons in ESD Drd3::Cre mice restored the latency to make the first USV call (n = 7, 8 mice for each control group and n = 8, 11 mice for ESD group).

(G) Schematics for the intraperitoneal injections of the saline or PD128907 to wild-type mice (left). Representative images of c-fos staining in the LS of control and ESD mice following saline or PD128907 injection (0.1 or 0.5 mg/kg, i.p.). Scale bars, 50 μm (right).

(H) Quantifications of c-fos-positive cells in the LS of control or ESD mice 1 h after saline or PD128907 administration. The high dose of PD128907 activated the LS neurons both in control and ESD mice (n = 3, 4 and 4 mice for each control group and n = 3, 3 and 6 mice for each ESD

group).

(I) Locations of the injection cannula tips in the mice included in Figure 5B. Symbols represent the different groups: white circle, saline; light green circle, PD128907 (0.1 μg/side); purple circle, PD128907 (2.5 μg/side).

(J) Representative images of c-fos immunoreactivity in the caudal LS where cannula tips were not placed. No changes were observed in the c-fos expression levels, regardless of drug treatments.

Significance for multiple comparisons: Two-way RM ANOVA; post-hoc, Fisher LSD [(E)], and Two-way ANOVA; post-hoc, Bonferroni [(F), (H)], $^{*}P < 0.05$; $^{**}P < 0.01$; $^{***}P < 0.001$; $^{\dagger}P < 0.05$; $^{\dagger\dagger\dagger}P < 0.001$. n.s., not significant. Data are presented as mean ± s.e.m.

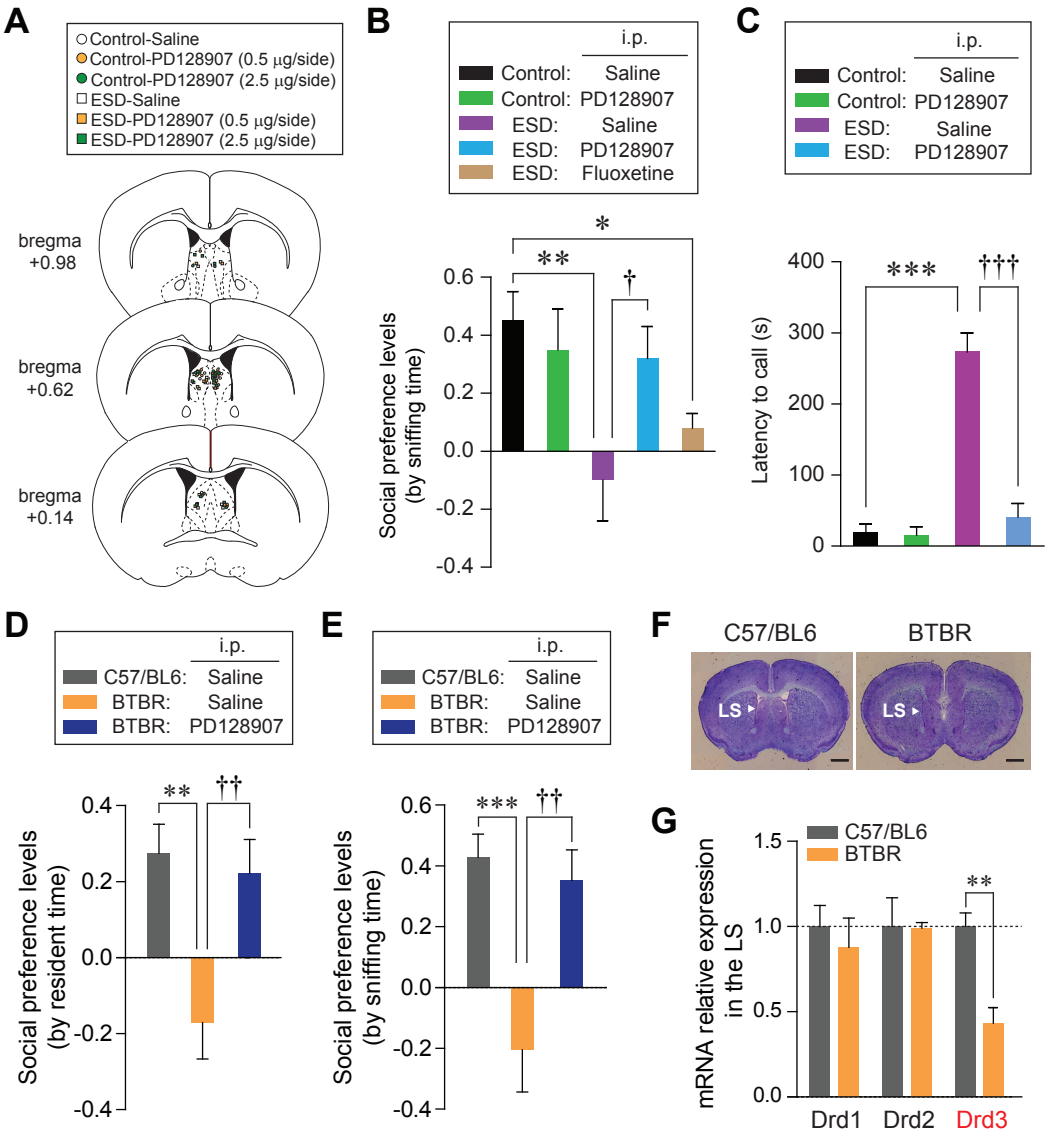
A
Control-Saline
Control-PD128907 (0.5 μg/side)
Control-PD128907 (2.5 μg/side)
ESD-Saline
ESD-PD128907 (0.5 μg/side)
ESD-PD128907 (2.5 μg/side)
bregma +0.98
bregma +0.62
bregma +0.14
B
i.p.
Control: Saline
Control: PD128907
ESD: Saline
ESD: PD128907
ESD: Fluoxetine
Social preference levels (by sniffing time)
C
i.p.
Control: Saline
Control: PD128907
ESD: Saline
ESD: PD128907
Latency to call (s)
D
i.p.
C57/BL6: Saline
BTBR: Saline
BTBR: PD128907
Social preference levels (by resident time)
E
i.p.
C57/BL6: Saline
BTBR: Saline
BTBR: PD128907
Social preference levels (by sniffing time)
F
C57/BL6
BTBR
LS
G
C57/BL6
BTBR
mRNA relative expression in the LS
Drd1
Drd2
Drd3

Figure S6

Figure S6. Administration of Drd3 Agonist, PD128907 (0.5 mg/kg, i.p.) Reverses Social Impairments in both ESD and BTBR mice, Related to Figure 6

(A) Locations of the injection cannula tips in the mice included in Figure 6C. Symbols represent the different groups: white circle, control-saline; yellow circle, control-PD128907 (0.5 μg/side); green circle, control-PD128907 (2.5 μg/side); white rectangle, ESD-saline; yellow rectangle, ESD- PD128907 (0.5 μg/side); green rectangle, ESD-PD128907 (2.5 μg/side).

(B) Social preference levels based on sniffing time in three-chamber test. PD128907 administration rescued impaired social preferences in ESD mice to the level of control mice, whereas chronic fluoxetine did not (n = 6, 5 mice for each control group, n = 6, 6 and 5 mice for each ESD group).

(C) PD128907 administration restored the latency to produce the first USV call emitted by ESD mice (n = 5, 6 mice for each control group, n = 6, 6 mice for each ESD group).

(D and E) PD128907 administration rescued impaired social preference of BTBR mice, a traditional animal model of ASD, based on resident time (D) and on sniffing time (E) in three-chamber test (n = 10 mice for C57/BL6 group, n = 8, 8 mice for each BTBR group).

(F) Representative images of coronal brain slices showing the LS of C57/BL6 (left) and BTBR mice (right). Scale bars, 1 mm.

(G) qRT-PCR analysis of Drd3 mRNA expression from the LS of C57/BL6 versus BTBR mice (n = 5 mice for C57/BL6 group, n = 4 mice for BTBR group).

Significance for multiple comparisons: One-way ANOVA; post-hoc, Fisher LSD [(B), (D), and (E)], Two-way ANOVA; post-hoc, Bonferroni [(C)], and Unpaired t-test [(G)], $^{*}P < 0.05$; $^{**}P < 0.01$; $^{***}P < 0.001$; $^{\dagger}P < 0.05$; $^{\dagger\dagger}P < 0.01$; $^{\dagger\dagger\dagger}P < 0.001$. Data are presented as mean ± s.e.m.

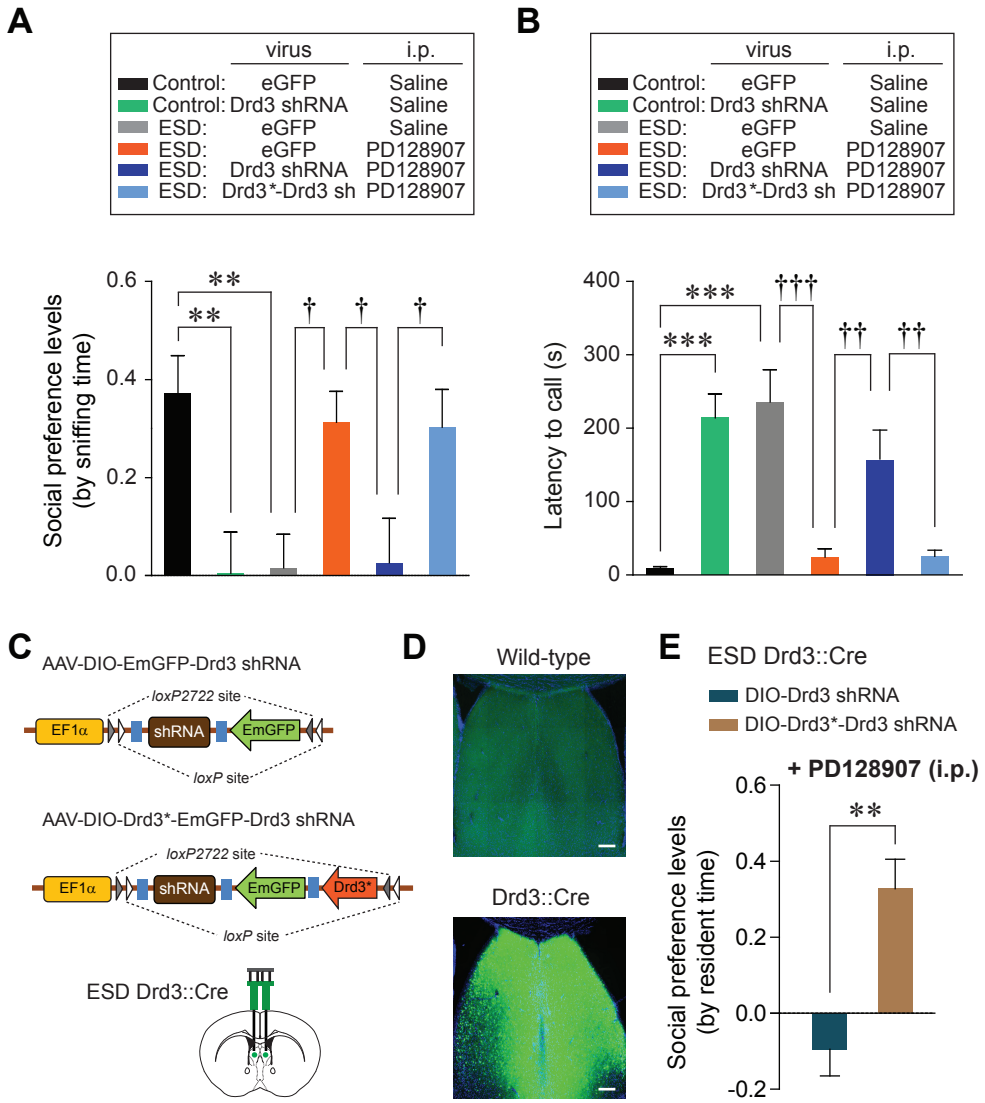
A
virus
i.p.
Control: eGFP Saline
Control: Drd3 shRNA Saline
ESD: eGFP Saline
ESD: eGFP PD128907
ESD: Drd3 shRNA PD128907
ESD: Drd3*-Drd3 sh PD128907
Social preference levels (by sniffing time)
0.6
0.4
0.2
0.0
**
**
†
†
†
B
virus
i.p.
Control: eGFP Saline
Control: Drd3 shRNA Saline
ESD: eGFP Saline
ESD: eGFP PD128907
ESD: Drd3 shRNA PD128907
ESD: Drd3*-Drd3 sh PD128907
Latency to call (s)
400
300
200
100
0
***
***
†††
††
††
C
AAV-DIO-EmGFP-Drd3 shRNA
loxP2722 site
EF1α
shRNA
EmGFP
loxP site
AAV-DIO-Drd3*-EmGFP-Drd3 shRNA
loxP2722 site
EF1α
shRNA
EmGFP
Drd3*
loxP site
ESD Drd3::Cre
D
Wild-type
Drd3::Cre
E
ESD Drd3::Cre
DIO-Drd3 shRNA
DIO-Drd3*-Drd3 shRNA
+ PD128907 (i.p.)
Social preference levels (by resident time)
0.6
0.4
0.2
0.0
-0.2
**

Figure S7

Figure S7. Administration of Drd3 Agonist, PD128907 (0.5 mg/kg, i.p.) Reverses ESD-Induced Social Impairments via Drd3^{LS} Neuronal Signaling, Related to Figure 6

(A and B) Knock-down of Drd3 by injection of AAV-Drd3-shRNA into the LS attenuated social preference levels based on sniffing time in three-chamber test (A) and delayed latency for making the first USV call (B) in control mice. It also blocked PD128907-induced rescue of social dysfunctions in ESD mice. However, the expression of shRNA-resistant Drd3 (Drd3*, mutant form is indicated by asterisk) together with shRNA against Drd3 (AAV-Drd3*-Drd3 sh) did not block PD128907-induced rescue of those social impairments in ESD mice. (A, n = 11, 10 mice for each control group, n = 9, 10, 11 and 11 mice for each ESD group). (B, n = 8, 10 mice for each control group, n = 7, 8, 9 and 10 mice for each ESD group).

(C) Schematic illustrating the bilateral injections of AAV expressing Drd3 shRNA or Drd3*-Drd3 shRNA in a Cre-dependent manner into the LS of ESD Drd3::Cre mice.

(D) Images of the Drd3*-EmGFP-Drd3 shRNA expression after bilateral injections of AAV-DIO-Drd3*-EmGFP-Drd3 shRNA into the LS of wild-type (top) and Drd3::Cre mice (bottom). Scale bars, 250 μm.

(E) Social preference levels based on resident time in three-chamber test. Selective expression of Drd3*-Drd3 shRNA in Drd3^{LS} neurons of ESD Drd3::Cre mice still did not preclude PD128907-induced rescue of impaired social preference (n = 4 mice per group).

Significance for multiple comparisons: One-way ANOVA; post-hoc, Fisher LSD [(A), (B)], Unpaired t-test [(E)], $^{**}P < 0.01$; $^{***}P < 0.001$; $^{\dagger}P < 0.05$; $^{\dagger\dagger}P < 0.01$; $^{\dagger\dagger\dagger}P < 0.001$. Data are presented as mean ± s.e.m.